



**HAL**  
open science

## **Distinct Patterns of Colocalization of the CCND1 and CMYC Genes With Their Potential Translocation Partner IGH at Successive Stages of B-Cell Differentiation**

Ilya Sklyar, Olga V. Iarovaia, Alexey A. Gavrilov, Andrey Pichugin, Diego Germini, Tatiana Tsfasman, Gersende Caron, Thierry Fest, Marc Lipinski, Sergey V. Razin, et al.

► **To cite this version:**

Ilya Sklyar, Olga V. Iarovaia, Alexey A. Gavrilov, Andrey Pichugin, Diego Germini, et al.. Distinct Patterns of Colocalization of the CCND1 and CMYC Genes With Their Potential Translocation Partner IGH at Successive Stages of B-Cell Differentiation. *Journal of Cellular Biochemistry*, 2016, 117 (7), pp.1506-1510. 10.1002/jcb.25516 . hal-01295670

**HAL Id: hal-01295670**

**<https://univ-rennes.hal.science/hal-01295670>**

Submitted on 14 Jun 2016

**HAL** is a multi-disciplinary open access archive for the deposit and dissemination of scientific research documents, whether they are published or not. The documents may come from teaching and research institutions in France or abroad, or from public or private research centers.

L'archive ouverte pluridisciplinaire **HAL**, est destinée au dépôt et à la diffusion de documents scientifiques de niveau recherche, publiés ou non, émanant des établissements d'enseignement et de recherche français ou étrangers, des laboratoires publics ou privés.

**Distinct patterns of colocalization of the *CCND1* and *CMYC* genes with their potential translocation partner *IGH* at successive stages of B-cell differentiation.**

Ilya Sklyar<sup>1,2,3</sup>, Olga V. Iarovaia<sup>1,2,3</sup>, Alexey A. Gavrilov<sup>2,3</sup>, Andrey Pichugin<sup>1,2</sup>, Diego Germini<sup>1,2</sup>, Tatiana Tsfasman<sup>1,2</sup>, Gersende Caron<sup>4</sup>, Thierry Fest<sup>4</sup>, Marc Lipinski<sup>1,2</sup>, Sergey V. Razin<sup>2,3,5,6</sup>, and Yegor S. Vassetzky<sup>1,2,5,6</sup>

<sup>1</sup>UMR8126, CNRS, Université Paris-Sud, Institut de Cancérologie Gustave Roussy, Villejuif, France

<sup>2</sup>LIA1066 « Laboratoire Franco-Russe de Recherche en Oncologie »

<sup>3</sup>Institute of Gene Biology, Russian Academy of Sciences, Moscow, Russia

<sup>4</sup>INSERM U917, Université de Rennes, Rennes, France

<sup>5</sup>Faculty of Biology, M.V. Lomonosov Moscow State University, 119992 Moscow, Russia

<sup>6</sup>Corresponding author:

Tel: +33(0)1 42 11 62 83

Fax: +33(0)1 42 11 54 94

Email: vassetzky@igr.fr

## ABSTRACT

The immunoglobulin heavy chain (*IGH*) locus is submitted to intra-chromosomal DNA breakages and rearrangements during normal B cell differentiation that create a risk for illegitimate inter-chromosomal translocations leading to a variety of B-cell malignancies. In most Burkitt's and Mantle Cell lymphomas, specific chromosomal translocations juxtapose the *IGH* locus with a *CMYC* or Cyclin D1 (*CCND1*) gene, respectively. 3D-fluorescence in situ hybridization was performed on normal peripheral B lymphocytes induced to mature in vitro from a naive state to the stage where they undergo somatic hypermutation (SHM) and class switch recombination (CSR). The *CCND1* genes were found very close to the *IGH* locus in naive B cells and further away after maturation. In contrast, the *CMYC* alleles became localized closer to an *IGH* locus at the stage of SHM / CSR. The colocalization observed between the two oncogenes and the *IGH* locus at successive stages of B-cell differentiation occurred in the immediate vicinity of the nucleolus, consistent with the known localization of the RAGs and AID enzymes whose function has been demonstrated in *IGH* physiological rearrangements. We propose that the chromosomal events leading to Mantle Cell lymphoma and Burkitt's lymphoma are favored by the colocalization of *CCND1* and *CMYC* with *IGH* at the time the concerned B cells undergo VDJ recombination or SHM/CSR, respectively.

**Keywords:** nuclear organization, B-cell lymphoma, illegitimate recombination, *IGH*, *CMYC*, *CCND1*

## INTRODUCTION

A variety of lymphomas and leukaemias are associated with specific chromosomal translocations. Immunoglobulin genes submitted to maturation during physiological B-cell differentiation are prone to illegitimate chromosomal rearrangements and B-cell transformation (reviewed in <sup>1</sup>). Antibodies result from the assembly of light and heavy polypeptide chains, each submitted to a multistep process including intrachromosomal rearrangements and mutagenesis events that take place along B-cell differentiation. The 14q subtelomeric immunoglobulin heavy chain (*IGH*) locus is made of 123 to 129 variable (V), 27 diversity (D), 9 joining (J) and 11 constant (C) coding segments. The antibody repertoire originates from V(D)J recombination events taking place in the bone marrow and resulting in the juxtaposition of one V, one D, and one J segment in a process that is catalysed by the recombination-activating enzymes *RAG1* and *RAG2* <sup>2</sup>. The antibody affinity is further modified by somatic hypermutation (SHM) in lymph nodes under the action of the AID (activation-induced DNA-cytosine deaminase) enzyme. Finally and also relying on AID, the antibody isotype is defined by class switch recombination (CSR) between constant region segments <sup>3</sup>.

It is generally assumed that inter-chromosomal translocations result from an erroneous repair of DNA double-strand breaks (DSB) in two different chromosomes that happen to be positioned next to each other in the nuclear space. Mantle cell lymphoma (MCL) and Burkitt's lymphoma (BL) are two examples of B-cell proliferations associated with specific chromosomal translocations involving the *IgH* locus on chromosome 14q. Following the translocation, the *IGH* locus ends up juxtaposed on the rearranged chromosome 14q+ with either the cyclin D1 gene (*CCND1*) or the *CMYC* oncogene in MCL and BL, respectively. We

have recently reported <sup>4</sup> that in cell-lines derived from MCL or BL, one allele of *CCND1* (in MCL) or *CMYC* (in BL) is positioned statistically farther from the nuclear membrane and closer to the outer surface of the nucleolus than in their non-malignant counterparts. In this new nuclear position rich in RNA polymerase II, they become accessible to, and are positively regulated by, the abundant nucleolus-derived transcription factor nucleolin. While the-MCL specific translocation occurs in the bone marrow at an early stage of B-cell differentiation at the time of V(D)J recombination, the BL-specific translocation occurs in a lymph node in a more differentiated B cell that has already undergone VDJ recombination and is submitted to SHM and CSR <sup>5-7</sup>. Since RAGs and AID have been reported to be also associated with the nucleolus <sup>8,9</sup>, we postulated that the *IGH*, *CCND1* or *CMYC* loci could be positioned sufficiently close to each other that the probability would be increased of DSBs occurring not only within the physiological *IgH* target, but also within or next to *CCND1* (on chromosome 11q) or *CMYC* (on 8q). This would then open the way to illegitimate non-homologous end joining (NHEJ; reviewed in <sup>10</sup>) leading to a t(11;14) MCL- or t(8;14) BL-associated translocation. Indeed, a spatial proximity between *CMYC* and *IGH* was previously observed upon activation of murine B lymphocytes <sup>11</sup> and in human B-cells <sup>12</sup>.

## RESULTS AND DISCUSSION

We postulated that the *IGH*, *CCND1* or *CMYC* loci could be positioned close to each other at different stages of B-cell maturation. To substantiate this hypothesis, we have used an inducible system of *in vitro* human B-cell maturation recently developed by Fest and collaborators<sup>13</sup>. In short, naive B-cells isolated from peripheral blood are first activated to proliferate for four days followed by treatment with a cocktail of IL-2, IL-6, IL-10 and IL-15. Cells are harvested at day 5 when SHM and CSR take place (see supplementary Materials and Methods). Using 3D-FISH and computer analysis, we have measured the distances between a) the *CMYC* or *CCND1* oncogenes and the nearest *IGH* allele, and b) the distance of the considered oncogene to the surface of the nearest nucleolus. The raw data are presented in Table S1. Scatterplots exhibited in Figure 1 represent results compiled from two independent experiments and indicate that in naive B cells, a correlation exists between the distances from either oncogene to the *IgH* locus on one hand (X axis) and to the nucleolus on the other hand (Y axis) and this applies to both *CMYC* ( $p=1\times 10^{-8}$ , Figure 1A) and *CCND1* ( $p=1\times 10^{-5}$ , Figure 1C). At the stage of SHM/CSR, the correlation holds true for *CMYC* (Figure 1B,  $p=6\times 10^{-6}$ ) but not for *CCND1* (Figure 1D,  $p=0.03$ ). We have used the human beta-globin gene locus located on chromosome 11p as an unrelated control. We did not find any change in its intranuclear localization between naive and SHM/CSR B-cells (Table S1, Figure S2).

Since genomic loci are more likely to participate in a chromosomal translocation event when positioned closer to each other, we next decided to differentiate our observations according to whether the considered *CMYC* or *CCND1* allele was the allele closer (*IGH*-proximal) or more distant (*IGH*-distal) to the *IGH* locus (Figure 2A,B). Average distances to the nucleolus

were then calculated. As seen in Figure 2C, the *CMYC* distance to the nucleolus was significantly higher in naive B cells than at the SHM/CSR stage and this was true for both the *IGH*-proximal (blue,  $p=3\times 10^{-6}$ ) and *IGH*-distal (yellow,  $p=1\times 10^{-5}$ ) alleles. In contrast, and as expected, the distances of *CCND1* to the surface of the nucleolus was significantly larger at the SHM/CSR stage as compared with naive B cells and again, this was the case for both alleles (Figure 2C,  $p=1\times 10^{-23}$  and  $1\times 10^{-19}$ ). When the two experiments compiled in Figures 1 and 2 were analyzed separately, the results were very similar as seen in Figure S1. Of note, whereas the two *CMYC* alleles behaved differently from one another, one being consistently and significantly closer to the nucleolus than the other ( $p=0.03$  in naive B cells and  $9\times 10^{-3}$  at the SHM/CSR stage), there was little difference between the two *CCND1* alleles in their relative distance to the nucleolus at either stage of differentiation (Figure 2C). In fact, both *CCND1* loci were located very close to the nucleolar periphery (less than  $0.5\ \mu\text{m}$  in most cases) in naive B-cells, and considerably farther away at the SHM/CSR stage. Also of note is the observation that the size of the nuclei did not vary significantly between the naive and SHM/CSR stages of B cell differentiation (Figure 2D). Thus, the respective distances between the oncogenes and the nucleolus cannot be accounted for by differences in the nuclear volume at different stages of differentiation. Collectively, our data thus demonstrate that in the course of B-cell differentiation from a naive state to the stage of SHM and CSR, the *CMYC* and *CCND1* alleles are submitted to opposite movements, the former moving closer to, the latter away from, the nucleolus.

It is known that the MCL-specific t(11;14) translocation that juxtaposes one *CCND1* allele next to an *IGH* locus occurs during V(D)J recombination at an early stage of B-cell differentiation<sup>14</sup>, i.e. earlier than the (8;14) translocation that brings a *CMYC* allele next to an *IGH* locus as seen specifically in BL. This is consistent with the present observation that

*CCND1* loci lie closer to the nucleolus in naive than in matured B cells and with the fact that the correlation with their proximity to an *IGH* locus was observed only in naive B-cells. The situation is different for the BL-associated translocation which occurs in B-cells that have already undergone V(D)J recombination in the bone marrow before they enter the blood circulation where they do not replicate their DNA and hence do not divide. As it is known that the major changes in nuclear architecture occur during cell division and differentiation<sup>15</sup>, it is very likely that the nuclear positioning of the genes observed in naive B-cells represents a snapshot of the nuclear organization at the time of V(D)J recombination. During activation in lymph nodes, B-cells undergo several rounds of cell division, their nuclear architecture being modified to prepare for SHM and CSL and they become susceptible to a BL-associated chromosomal translocation. Thus, the perinucleolar localization of *CCND1* and *CMYC* observed at successive stages of B-cell differentiation as reported here could explain the mechanism of transformation leading to MCL and BL, respectively. Similar mechanisms may be implicated in the generation of other lymphomas associated with specific chromosomal translocations involving immunoglobulin genes.



## METHODS

***In vitro* B-cell differentiation.** Peripheral blood cells from healthy volunteers were obtained from the French Blood Center. Naive B cells (Day<sub>0</sub>; CD19+CD27-) were purified from peripheral blood mononuclear cells by depletion with magnetic beads (naive B cell isolation kit II, Miltenyi Biotech). Then the cells were activated in RPMI 1640 (Invitrogen) supplemented with 10% FCS and antibiotics (Invitrogen). Purified B-cells were cultured at  $7.5 \cdot 10^5$  cells/ml in 24-well plates and stimulated during 4 days with 2  $\mu$ g/ml F(ab')<sub>2</sub> Fragment Goat Anti-Human IgA+IgG+IgM (H+L) (Jackson ImmunoResearch Laboratories, West Grove, PA), 50 ng/ml recombinant human soluble CD40L associated with 5  $\mu$ g/ml cross-linking Ab (R&D Systems, Abingdon, United Kingdom), 2.5  $\mu$ g/ml CpG oligodeoxynucleotide 2006 (Cayla Invivogen, Toulouse, France) and 50 U/ml recombinant IL-2 (SARL Pharmaxie, Aigueperse, France). To initiate plasmablast generation, the cells were harvested at Day<sub>4</sub>, washed, and seeded at  $4 \times 10^5$ /ml with IL-2 (50 U/ml), IL-4 (10 ng/ml), and IL-10 (10 ng/ml) (R&D Systems). Mature plasmocytes were isolated from peripheral blood using the CD138+ Plasma Cell Isolation Kit (Miltenyi Biotech) .

### **Three-Dimensional Fluorescence In Situ Hybridization (3D-FISH) and Immuno-**

**detection.** Cells were immobilized on Cell-Tak (BD Biosciences, Bedford, MA)-coated glass coverslips. The slides were then treated as described previously to preserve their 3D structure<sup>16</sup>. Denatured nuclei were hybridized overnight with denatured probes. The probes were purchased stained from Blue Gnome (Cambridge, UK). After probe hybridization, slides were washed according to the manufacturer's protocol. Nucleoli were detected using mouse anti-B23 antibody (Sigma, St Louis, MO) and chicken anti-mouse Alexa 647 (Molecular Probes, Carlsbad, CA).

**Confocal Microscopy.** Nuclei were scanned with an axial distance of 100 nm using a laser scanning confocal microscope (Zeiss LSM 510, Zeiss, Oberkochen, Germany). Stacks of gray-scale two-dimensional images were obtained with a pixel size of 47 nm. Displayed overlays of confocal images were processed as described elsewhere <sup>4</sup>.

**Image Processing, Measurements and Statistical Analysis.** The images obtained using Zeiss LSM 510 were analyzed using semi-automated image processing and analysis tools <sup>17,18</sup>. Images were automatically resized to a constant voxel size (0.99x0.99x0.512  $\mu\text{m}$ ) and processed to get segmented, labeled objects. Segmented nuclei defined the regions of interest in the 3D data sets. A 3D binary mask was first determined by a threshold method: it analyzes only the background intensities and assigns the intensity value [mean + f \* sigma] as the lower threshold. The weighting factor f (3 to 10) was applied as the signal-to-noise ratio (SNR) in each cell type. Next, nuclei were extracted from the binary mask with an a priori method based on their size and shape: a combination of 2D and 3D attribute opening transformations was applied to remove the smallest objects. Connected voxels representing nuclei were then identified with label object representation and manipulation filters; 3D morphological opening and closing transformations were applied to fill and smooth the rough labeled objects. Finally, the bounding box of each nucleus was used to crop smaller 3D data sets in the color channels of immunoglobulin heavy chain gene, the oncogene of choice and nucleoli, and to determine radial position of gene in nuclear volume.

Gene alleles were detected using an automatic threshold segmentation procedure with subsequent subtraction of a background image generated by a three-dimensional median filtering and morphological top-hat transformation. The gene signals appeared spherical.

Binary masks containing these structures were produced from cropped images for segmentation. Independent objects were generated from label-connected binary voxels. The not biologically pertinent objects were removed. The selection process was used: first, the segmented alleles were included into the study when the labeled objects were bigger than  $0.4 \mu\text{m}^3$  and smaller than  $2.0 \mu\text{m}^3$ . Second, when the number of labeled objects in one nucleus was less than 2 (corresponds to number of gene alleles in diploid chromosome set before replication) all nuclei were removed. For naïve B-lymphocytes, the nuclei were removed when the number of labeled objects in one nucleus was greater than 4 (corresponds to number of gene alleles in diploid chromosome set after replication). For lymphoma cells, the nuclei were removed when the number of labeled objects in one nucleus was greater than 6 (corresponds to number of gene alleles in rearranged genomes). The geometrical center of mass was calculated for each object.

Nucleoli were detected using automatic threshold segmentation as described above with the following modifications: nucleoli were extracted from the binary mask with an a priori method based on their size and shape. The objects smaller than  $0.23 \mu\text{m}^3$  were removed. The nucleoli with spherical or other shapes have been segmented using morphological erosion with a mild structuring element ( $3 \times 3 \times 3$  voxels) and labeling of connected voxels.

Bounding box was created for the segmented nucleoli in order to measure the distance from gene allele to nucleolus. The shortest length of the straight line from the center of mass of segmented allele to the bounding box of nucleolus was obtained for each allele. The alleles localized at the distance of  $1.0 \mu\text{m}$  to nucleolus or shorter were assumed as associated with nucleolus. Distributions were compared using the Student's t test.

## **Ethics Statement**

The human blood from healthy donors was purchased from the French Blood transfusion center in accordance to the French National legislation.

### **Acknowledgements**

This research was supported by the Russian Science Foundation, project #14-24-00022 to IS, OVI, AAG and SVR and by grants from INCa (ERABL) and ANRS (#1154) to YSV. AG is a fellow of Dmitri Zimin's Dynasty Foundation.

### **Author Contribution**

YSV, AP, OI designed research; AP, IS, DG, TT, OI performed research; AP, IS, AAG, OI, SVR, ML, YSV analyzed data; GL, TF contributed reagents; OI, SVR, AAG, ML, YSV wrote the paper.

### **Conflict of interest**

The authors declare no conflict of interest.

## Figure Legends

**Figure 1.** Distances between the *CMYC* / *CCND1* oncogene and the *IGH* locus are correlated with their proximity to the nucleolus. Scatterplots represent the relative distances of each *CMYC* (A, B) or *CCND1* (C, D) allele to the nearest *IGH* locus (X axis) and nucleolar surface (Y axis) as measured in the nucleus of naive B-cells (A, 128 nuclei analyzed; C, 136) or B cells at the stage of SHM/CSR (B, 131 nuclei; D, 143 nuclei). R, Pearson correlation coefficient. P, p-value calculated using the online p-Value Calculator for Correlation Coefficients, Soper D.S. (2015). (<http://www.danielsoper.com/statcalc3/calc.aspx?id=44>).

**Figure 2.** Separate observation of *IGH*-proximal and -distal *CMYC* and *CCND1* alleles with respect to the nucleolus. (A) Double-colored 3D DNA FISH for *IGH* (green) and *CMYC* (red) genes coupled with immunostaining of nucleoli (blue) on a B-cell at the SHM/CSR stage (superimposition with phase contrast image). (B) Schematic representation of *IGH*-proximal and -distal oncogene alleles. L1, the shortest distance between *IGH* and oncogene alleles. L2, distance between the other two *IGH* and oncogene alleles. (C) Boxplots of the distribution of oncogene distances to the nucleolus as indicated. (D) Boxplots of the distribution of nuclear diameters in naive and SHM/CSR B-cells (100 nuclei analyzed). P-values were calculated using two-tailed unpaired T-test. ns, non-significant.

**Figure S1.** (A) Separate representation of results from two independent experiments (rep 1 and rep 2). N, number of nuclei analyzed. P-values were calculated using two-tailed unpaired T-test. (B-C) Representative images of localization of *CCND1* and *IGH* loci in naive B-cells (B) and at the SHM/CSR stage (C). Red, *CCND1*, Green, *IGH*, Blue, B23 (nucleolus). Scale bar=5 $\mu$ M. (D-E) Representative images of localization of *CMYC* and *IGH* loci in naive B-

cells (D) and at the SHM/CSR stage (E). Red, CCND1, green, IGH, blue, B23 (nucleolus).  
Scale bar=5mM.

**Figure S2.** Distances between the *HBB* gene and the *IGH* locus at the naive and SHM/CSR stages of B cell differentiation. Boxplots represent the relative distances of each *HBB* allele to the nearest *IGH* locus in the nucleus of naive B-cells (left, 83 nuclei analyzed) or B cells at the stage of SHM/CSR (right, 65 nuclei analyzed). P-value was calculated using two-tailed unpaired T-test. ns, non-significant.

## REFERENCES

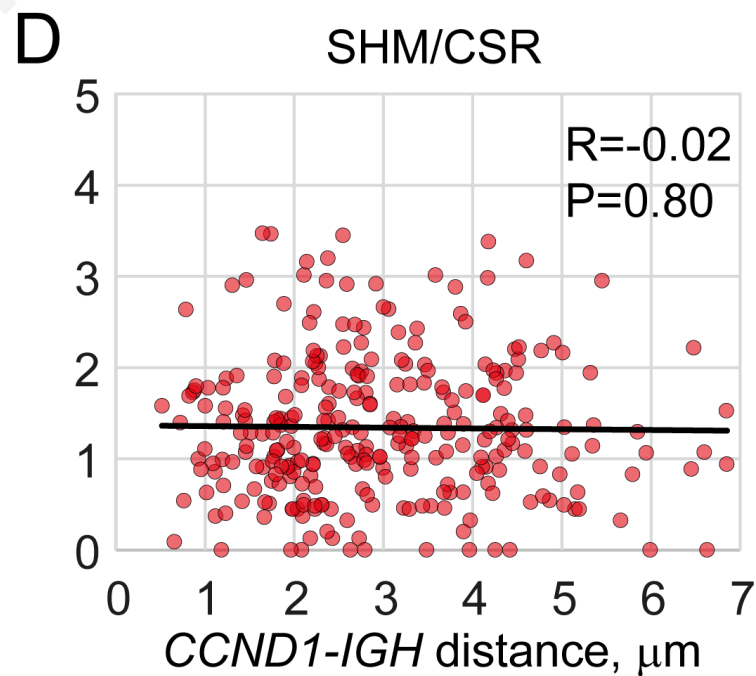
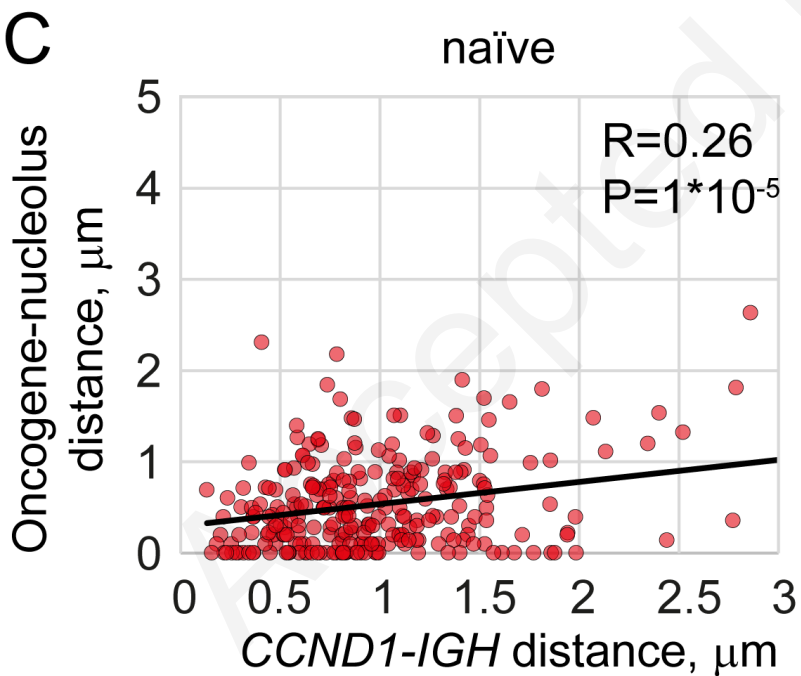
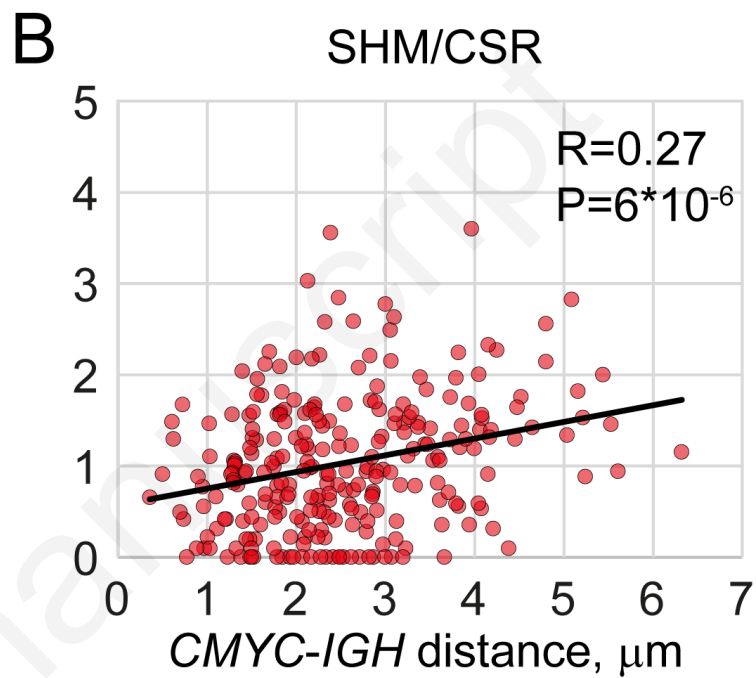
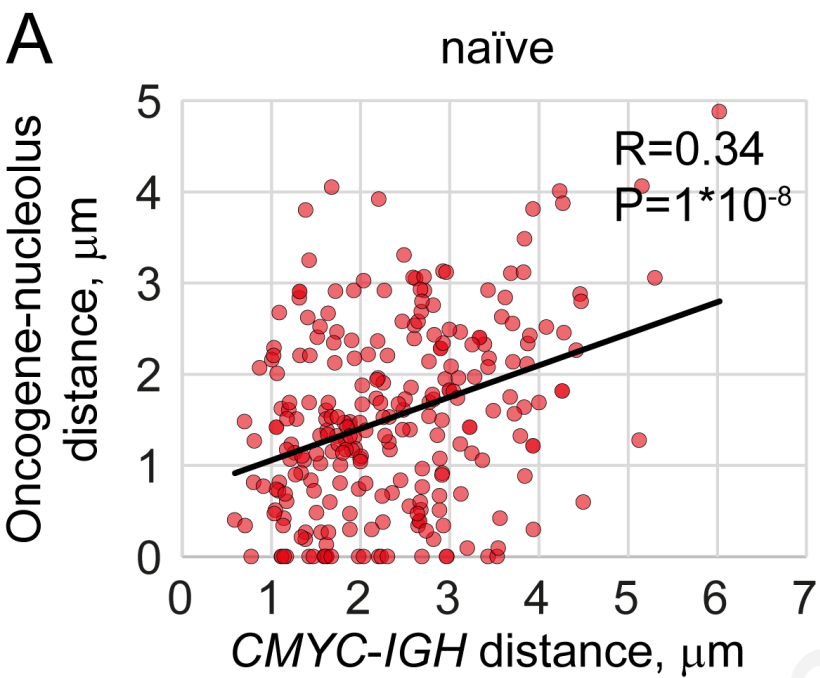
- 1 Sklyar I V., Iarovaia OI V., Lipinski M, Vassetzky YS. Translocations affecting human immunoglobulin heavy chain locus. *Biopolym Cell* 2014; **30**: 91–95.
- 2 Gellert M. V(D)J recombination: RAG proteins, repair factors, and regulation. *Annu Rev Biochem* 2002; **71**: 101–32.
- 3 Maizels N. Immunoglobulin gene diversification. *Annu Rev Genet* 2005; **39**: 23–46.
- 4 Allinne J, Pichugin A, Iarovaia O, Klibi M, Barat A, Zlotek-Zlotkiewicz E *et al.* Perinucleolar relocalization and nucleolin as crucial events in the transcriptional activation of key genes in mantle cell lymphoma. *Blood* 2014; **123**: 2044–53.
- 5 Bross L, Fukita Y, McBlane F, Démollière C, Rajewsky K, Jacobs H. DNA double-strand breaks in immunoglobulin genes undergoing somatic hypermutation. *Immunity* 2000; **13**: 589–597.
- 6 Schrader CE. Inducible DNA breaks in Ig S regions are dependent on AID and UNG. *J Exp Med* 2005; **202**: 561–568.
- 7 Stavnezer J, Schrader CE. IgH Chain Class Switch Recombination: Mechanism and Regulation. *J Immunol* 2014; **193**: 5370–5378.
- 8 Spanopoulou E, Cortes P, Shih C, Huang CM, Silver DP, Svec P *et al.* Localization, interaction, and RNA binding properties of the V(D)J recombination-activating proteins RAG1 and RAG2. *Immunity* 1995; **3**: 715–26.

- 9 Hu Y, Ericsson I, Torseth K, Methot SP, Sundheim O, Liabakk NB *et al.* A combined nuclear and nucleolar localization motif in activation-induced cytidine deaminase (AID) controls immunoglobulin class switching. *J Mol Biol* 2013; **425**: 424–43.
- 10 Iarovaia O V, Rubtsov M, Ioudinkova E, Tsfasman T, Razin S V, Vassetzky YS. Dynamics of double strand breaks and chromosomal translocations. *Mol Cancer* 2014; **13**: 249.
- 11 Osborne CS, Chakalova L, Mitchell JA, Horton A, Wood AL, Bolland DJ *et al.* Myc dynamically and preferentially relocates to a transcription factory occupied by Igh. *PLoS Biol* 2007; **5**: e192.
- 12 Roix JJ, McQueen PG, Munson PJ, Parada LA, Misteli T. Spatial proximity of translocation-prone gene loci in human lymphomas. *Nat Genet* 2003; **34**: 287–291.
- 13 Le Gallou S, Caron G, Delaloy C, Rossille D, Tarte K, Fest T. IL-2 requirement for human plasma cell generation: coupling differentiation and proliferation by enhancing MAPK-ERK signaling. *J Immunol* 2012; **189**: 161–73.
- 14 Jares P, Colomer D, Campo E. Molecular pathogenesis of mantle cell lymphoma. *J Clin Invest* 2012; **122**: 3416–3423.
- 15 Walter J, Schermelleh L, Cremer M, Tashiro S, Cremer T. Chromosome order in HeLa cells changes during mitosis and early G1, but is stably maintained during subsequent interphase stages. *J Cell Biol* 2003; **160**: 685–697.
- 16 Solovei I, Walter J, Cremer M, Habermann FA, Schermelleh L, Cremer T. FISH: A Practical Approach. In: Squire J, Beatty B, Mai S (eds). *FISH: A Practical Approach*. Oxford Univ. Press: Oxford, 2002.

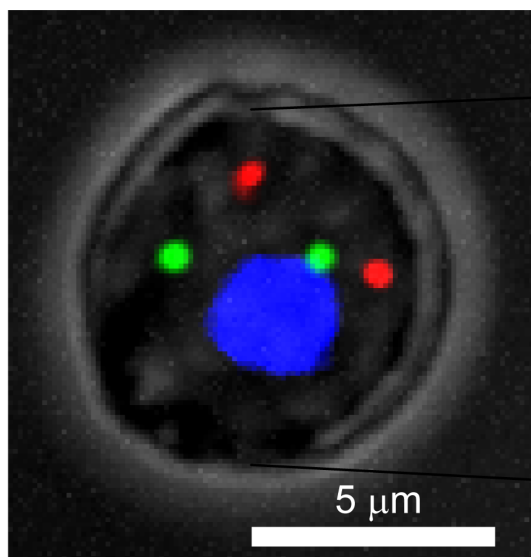


- 17 Pichugin A, Beaujean N, Vignon X, Vassetzky Y. Ring-like distribution of constitutive heterochromatin in bovine senescent cells. *PLoS One* 2011; **6**: e26844.
- 18 Aguirre-Lavin T, Adenot P, Bonnet-Garnier A, Lehmann G, Fleurot R, Boulesteix C *et al.* 3D-FISH analysis of embryonic nuclei in mouse highlights several abrupt changes of nuclear organization during preimplantation development. *BMC Dev Biol* 2012; **12**: 30.

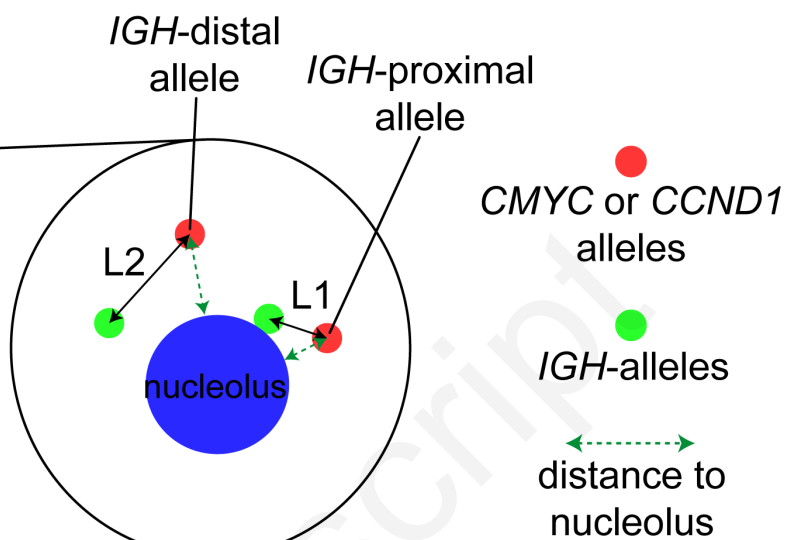
Accepted manuscript



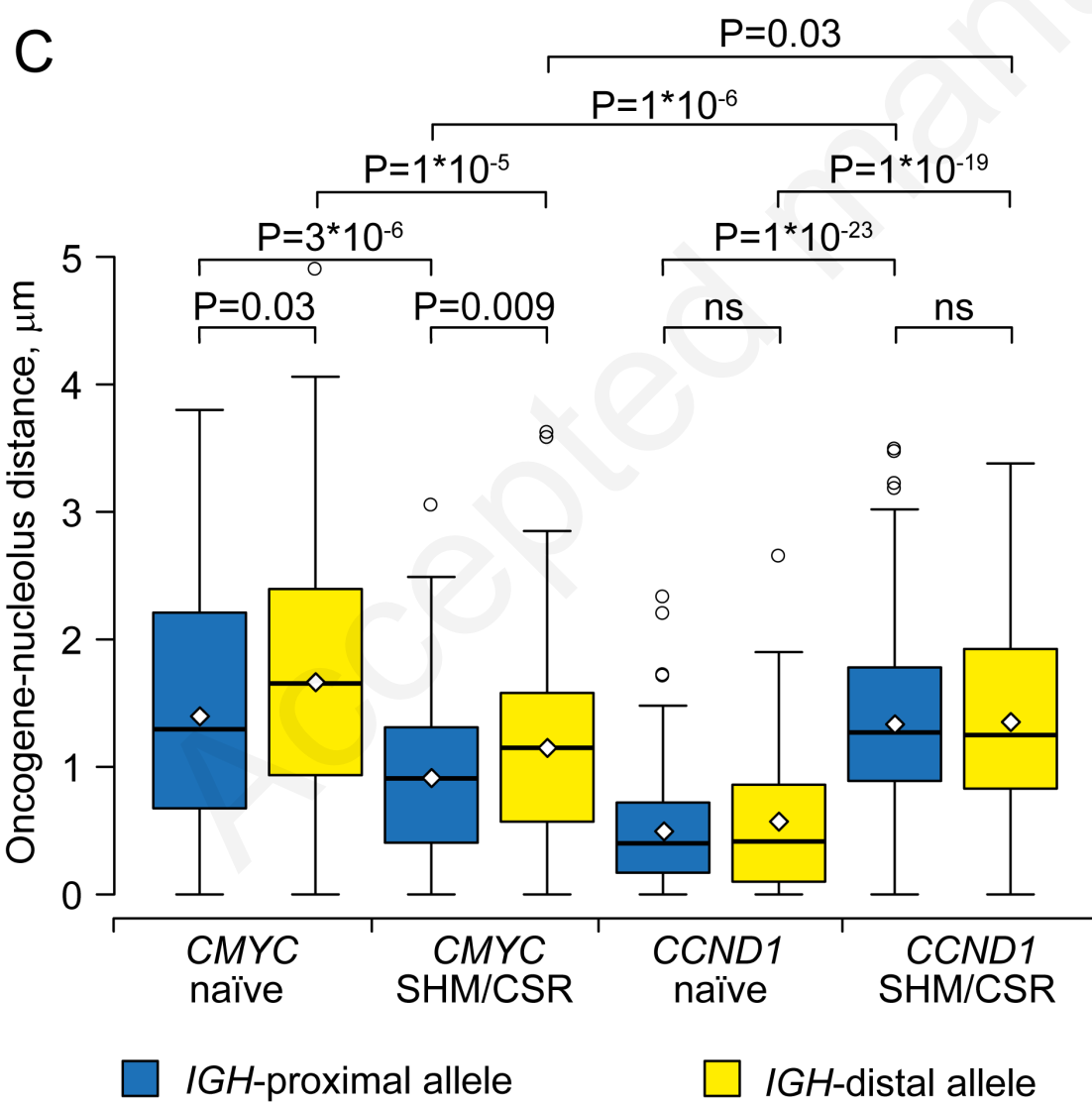
A



B



C



D

